Journal of Materials Chemistry A

Accepted Manuscript

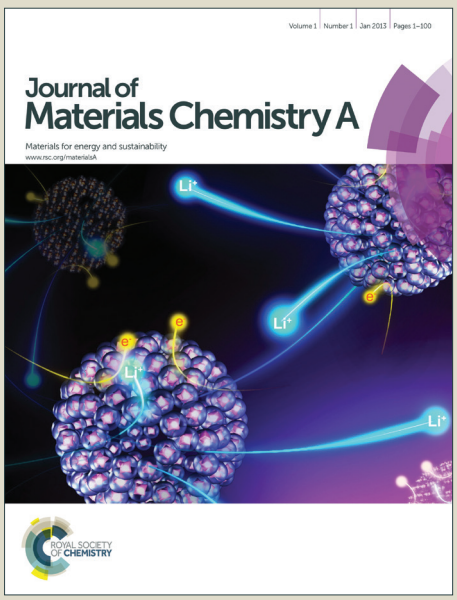

ROYAL SOCIETY OF CHEMISTRY

www.rsc.org/materialsA

Journal of Materials Chemistry

Cite this: DOI: 10.1039/c0xx00000x

www.rsc.org/xxxxxx

COMMUNICATION

Graphene wrapped chromium-MOF(MIL-101)/sulfur composite for performance improvement of high-rate rechargeable Li-S batteries

Zhenxia Zhao,*[a] Shao Wang,[b,c] Rui Liang,[b] Zhong Li,[c] Zhicong Shi[b] and Guohua Chen*[b]

Received (in XXX, XXX) Xth XXXXXXXXX 20XX, Accepted Xth XXXXXXXXX 20XX

DOI: 10.1039/b000000x

Graphene/chromium-MOF(MIL-101) composite is first proposed to serve as sulfur host for the stabilized Li-S batteries. The unique structure with high specific area and conductive shell ensures a high dispersion of sulfur in the composite and minimizes loss of polysulfide to the electrolyte.

With increase of global demand and environment crisis,[1] intense research on the design of advanced materials for energy storage systems have simulated and attracted much attention.[2] Among which, elemental sulfur has a high theoretical specific capacity of 1675 mA h g^{-1} against lithium and a specific energy of 2600 W h kg^{-1}.[3] Besides, sulfur has other advantages including high natural abundance, environmental friendliness and low cost. Hence, it will become the one of the most promising cathode materials for next generation energy storage systems.[4] However, despite of these promises, several key issues exist in Li-S batteries that hindered their commercial application in the cathode technology, involving their capacity fading, low active-material utilization and poor cathode conductivity.[5] Most of these problems are mainly caused by the inherent insulation and shuttling of high-order polysulfides intermediates in the electrolyte.[6]

Recently, some smart sulfur cathode configurations have been designed utilizing carbon or conducting polymer media to improve the capacity and cycle stability of sulfur cathodes, such as hollow carbon nanofiber,[7] CNT and graphene,[8,9] and porous carbon.[10] Among these composite preparations, adsorption can become an effective technique to infiltrate sulfur into porous hosts with very simple procedures.[10,11] Porous materials are the key factor in this technique. Metal organic frameworks (MOFs), an intriguing family of hybrid porous materials, have attracted increasing attention as gas adsorbents, sensors and catalysts materials owing to the extra high surface area, pore volume and tunable opening.[12] Hence, Tarascon and Ferey proposed MIL-100 to be a host for sulfur impregnation by using its mesopores with micro-aperture windows and improve the cycling capability of MIL-100@S composite cathod.[13] To improve the conductivity of the whole sulfur cathode, Zhang and Wu prepared the metal organic framework-derived porous carbons as sulfur host. They reported that the encapsulation of sulfur into metal organic framework-derived porous carbon improved the conductivity and limited the rapid capacity fading of prepared sulfur cathode as well.[14, 15] Moreover, the use of graphene coating for sulfur/sulfur-containing active materials have been well documented in recent works. Yang J. and Tu J.P. used graphene to modify the mesoporous carbon /sulfur composite (RGO@CMK-3/S), and improved the cycling stability and coulombic efficiency of the Li-S batteries.[16,17] Zhang Z. A. confined sulfur in mesoporous MOFs@reduced graphen oxide to construct a conductive network for the whole sulfur cathode.[18] Chen G.H. and Zhang Q. use graphene to wrap the sulfur and prepared the GES-sulfur core-shell structure to alleviate the polysulfide shuttle phenomenon.[19, 20]

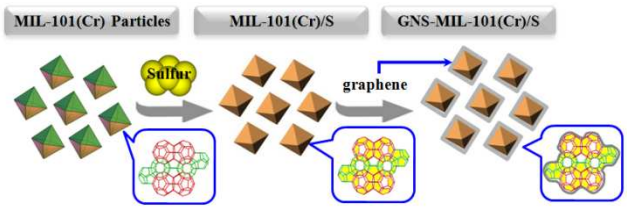

Fig. 1 Schematic illustration of the assembled GNS-MIL-101(Cr)/S composite for improving cathode performance. Sulfur was infiltrated into the MIL-101(Cr) using melting-diffusion route; graphene wrapping on the surface of the MIL-101(Cr)/S through the strong electrostatic attraction could effectively enhance the cathode's conductivity as well as immobilize the polysulfides dissolution in the electrolyte.

Here, MIL-101(Cr) is tried to propose as the sulfur host for the Li-S batteries. MIL-101 (Fig. S1, ESI†)[21] possesses much larger surface area (5000 m^2 g^{-1}) and pore volume (> 1.6 cm^3 g^{-1}) compared with MIL-100. The unique pore structure and high surface area will favor the high dispersion of sulfur into the pores with strong interaction. Moreover, graphene is used to wrap the MIL-101(Cr)/S composite in order to build a conductive bridge for electron transfer as well as a physical barrier to retard polysulfides dissolution into the liquid electrolyte. Fig. 1 illustrates the synthesis of a GNS-MIL-101(Cr)/S composite by a two-step approach. The prepared GNS-MIL-101(Cr)/S composite cathode possesses a much better capture of the polysulfides and

high electron conductivity, thus improving the cycling stability and rate capability as shown subsequently.

SEM (Fig. 2a and Fig. 2S ESI†) and TEM (Fig. 3S ESI†) images acquired from the GNS-MIL-101(Cr)/S composite display that most of the MIL-101(Cr) particles were covered with the thin wrinkled graphene veils uniformly and tightly. Moreover, the wrapped MIL-101(Cr)/S particles (Fig. 2a inset) preserve a similar morphology and particle size to the synthesized MIL-101 without any agglomeration of bulk sulfur on the particle surface. This indicates a high dispersion of sulfur into the porous framework matrix and a successful graphene wrapping on the MIL-101(Cr)/S composite. XRD patterns of the MIL-101(Cr) before and after sulfur infusion are almost similar to each other and no peak hints at the existence of sulfur crystal (Fig. 2b). It can be seen that sulfur in the MIL-101(Cr) may be amorphous or microcrystalline that cannot be detected by XRD.[22] Herein, combined with the SEM analysis, it can be deduced that sulfur is reduced to nano-particles and dispersed uniformly into the MIL-101(Cr) by melting route.

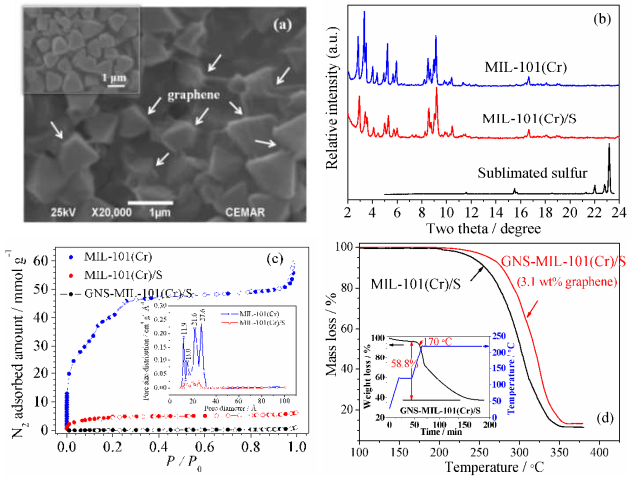

Fig. 2 (a) SEM images of the GNS-MIL-101(Cr)/S composite and the MIL-101(Cr)/S composite (inset); (b) X-ray diffraction patterns of sublimated surfur, the MIL-101(Cr) and the MIL-101(Cr)/S composite; (c) Nitrogen adsorption /desorption and pore size distribution (inset) of the MIL-101(Cr), the MIL-101(Cr)/S and the GNS-MIL-101(Cr)/S composites; (d) TG curve of the MIL-101(Cr)/S composite with and without graphene wrapping (S content: ~58.8% in the GNS-MIL-101(Cr)/S composite).

N_2 adsorption isotherms and the pore size distribution (obtained by DFT model) of the MIL-101(Cr), the MIL-101(Cr)/S and graphene wrapped MIL-101(Cr)/S (GNS-MIL-101(Cr)/S) composite are shown in Fig. 2c. Sulfur infusion caused a dramatic decrease in the BET surface area (from 3483 to 399 $m^2 g^{-1}$) and the total pore volume (from 1.5 $cm^3 g^{-1}$ to 0.21 $cm^3 g^{-1}$) of the MIL-101(Cr). It indirectly proves that, when sulfur was infiltrated into the MIL-101(Cr), the pores were preferentially filled with nano-sized sulfur, rather than being blocked on the outer surface of the MIL-101(Cr) particles. After being coated by graphene, the surface area continuously reduced to less than 100 $m^2 g^{-1}$. As seen in Fig. 2a, graphene veils covered the MIL-101(Cr)/S composite and blocked its pores, resulting in the low surface area of the GNS-MIL-101(Cr)/S composite. Thermogravimetric analysis results show that the mass loss profile is mainly attributed to the release of sulfur confined within the GNS-MIL-101(Cr)/S composite before the decomposition of MIL-101(Cr). It shifted to higher temperature compared to that of sulfur in the MIL-101(Cr)/S composite. The higher evaporation temperature reveals a stronger interaction of sulfur with the MIL-101 after being wrapped by graphene sheets. Besides the sulfur evaporation, the mass loss in TGA curves over 280 °C corresponds to the decomposition of the MIL-101 crystals, which is finished completely at about 340-350 °C.[21] To obtain the exact sulfur content in the GNS-MIL-101(Cr)/S composite, temperature programming lower than the decomposition temperature was used to evaporate all sulfur in GNS-MIL-101(Cr)/S composite. The inset of Fig. 2d shows that the total sulfur content could be determined as ~ 58.8 wt% with about 3.1% of graphene on the surface (calculated based on about 27 wt% remaining weight of the MIL-101 crystals after fully decomposing[21]).

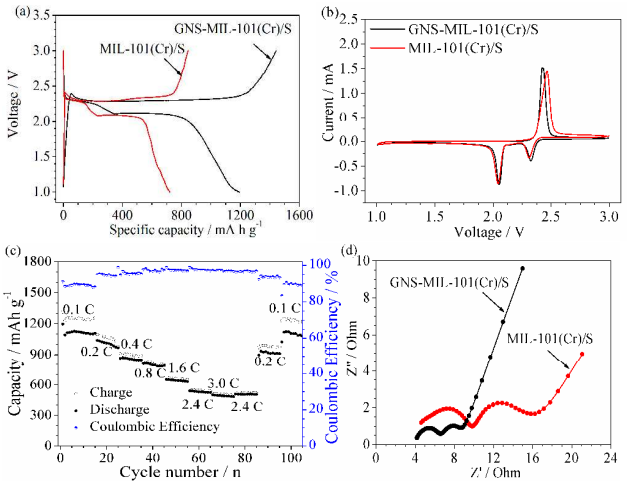

Fig. 3 Electrochemical characterization of the GNS-MIL-101(Cr)/S and MIL-101(Cr)/S composites (41.2 wt% sulfur in the electrode). (a) Charge and discharge voltage capacity profiles of these composites at a rate of 0.1 C; (b) Cyclic voltammetry curves of the GNS-MIL-101(Cr)/S and MIL-101(Cr)/S composite cathodes at scan rate of 0.1 mV s^{-1}; (c) Rate capability and coulombic efficiency of the GNS-MIL-101(Cr)/S composite cathode; (d) EIS plots of the GNS-MIL-101(Cr)/S and MIL-101(Cr)/S composite cathodes.

Fig. 3a shows the initial cycle voltage profiles of the MIL-101/S and graphene wrapped MIL-101/S cathodes at 0.1 C rate between 1.0 and 3.0 V. Two plateaus are clearly shown in all the discharge curves at 2.3 V and 2.1 V, corresponding to the formation of long-chain polysulfides (Li_2S_x, $4 \le x \le 8$) and then short-chain Li_2S_2 and Li_2S,[6] respectively. The cathode of the GNS-MIL-101(Cr)/S composite delivers much higher discharge capacity of 1192.5 mAh g^{-1} with smaller polarization (Fig. 3b) than the MIL-101(Cr)/S cathode (721.5 mA h g^{-1}). Although MIL-101 host has much lower electronic conductivity than carbon materials, they provide a huge surface area, which can improve the dispersion of sulfur homogeneously inside the pores. Meanwhile, the wrapping graphene serves as both the conductive network and containers to confine polysulfide species for the cathode. Thus, the discharge capacity and rate performance of the GNS-MIL-101(Cr)/S composite are dramatically enhanced in comparison to the MIL-101(Cr)/S composite (Fig. 3c and Fig.S5, ESI†). Also, as the current increases, the capacity of the GNS-MIL-101(Cr)/S decreases slowly from the reversible 1190 mA h

g^{-1} at 0.1 C to 1045, 870, 650 and 500 mA h g^{-1} at 0.2 C, 0.4 C, 0.8 C, 2.4 C and 3.0 C, respectively. Importantly, a reversible capacity of 1123 mA h g^{-1} is obtained when the current is switched back to 0.1 C, indicating a highly reversible, low capacity fading and efficient electrode enabled by the composite configuration of graphene wrapped high surface area framework host. The EIS of the two cathodes were measured and the results are given in Fig. 3d. The impedance spectra are all composed of two semicircles and an inclined line in their EIS spectra: the first semicircle at high frequency region is ascribed to lithium ion diffusion through the surface layer, and the second one at medium-to-low frequency region corresponds to the charge transfer and the inclined line in the low.[23] Clearly, graphene wrapped MIL-101(Cr)/S composite shows a much lower lithium ion diffusion and charge transfer resistance compared to the MIL-101(Cr)/S composite. Electrical measurements show that the GNS-MIL-101(Cr)/S has a conductivity of 0.10 S cm^{-1}, which is much higher than that of the MIL-101(Cr)/S composite (0.05 S cm^{-1}). It further confirms an improved ion/electron conductivities of the MIL-101(Cr)/S by wrapping graphene on the surface of MOF matrix.

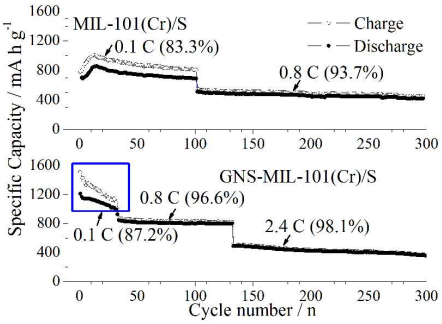

Fig. 4 Cycle performance and corresponding coulombic efficiency of the GNS-MIL-101(Cr)/S and MIL-101(Cr)/S composites under different current densities.

Cycling performance of the MIL-101(Cr)/S and GNS-MIL-100(Cr)/S composite cathodes at different current densities is shown in Fig. 4. The initial discharge capacity of MIL-101(Cr)/S composite is 715 mA h g^{-1}, and then gradually increased to 869 mA h g^{-1} at 0.1 C with ~ 83.3% coulombic efficiency. It retains a capacity of 695 mA h g^{-1} after 100 cycles with about 80% capacity retention. When the current increases to 0.8 C, its capacity is decreased to 512 mA h g^{-1} and only decreased by 19.9% over 300 cycles. The good cyclability can be attributed to the high interaction of sulfur and discharged polysulfides within the pores of the MIL-101 matrix. MIL-101 possesses the huge surface area and microporous aperture windows, which would supply abundant adsorption sites for sulfur as well as the polysulfides. Hence, it ensures a uniform dispersion of the sulfur with strong adsorption in the framework. Moreover, the larger cages would help to alleviate the deposition of the reduced lithium sulfides and to improve the penetration of electrolyte into the composite. However, the poor electron conductivity of the MIL-101 leads to a relative lower capacity compared to other carbon/S composite cathode.[2] After graphene wrapping on the surface of the MIL-101(Cr)/S composite, the capacity is increased to ~1200 mA h g^{-1} at 0.1 C rate. When increasing C-rate from 0.1 to 0.8 C, the GNS-MIL-101(Cr)/S maintains a reversible capacity of 847 mA h g^{-1} with 96.6% coulombic efficiency, followed by only 5.4% of capacity decrease from the 40th to the 134th cycles. At a high rate of 2.4 C, the GNS-MIL-101(Cr)/S composite is seen to deliver a discharge capacity of 497 mA h g^{-1} and maintains a reversible capacity of 395.9 mA h g^{-1} with 21% decrease over 300 cycles. Thus, both of the coulombic efficiencies and cycle stability at different C-rate are increased after being wrapped by graphene sheets. The improved electrochemical properties are mainly attributed to the formation of a 3-dimensional conducting network through the graphene nano-sheets.

Conclusions

In summary, MIL-101(Cr) with microporous windows and mesoporous cage is shown to be a good host for sulfur impregnation. Graphene wrapping on the MIL-101(Cr)/S composite has built a 3-D conducting network as well as a physical container, and thus dramatically enhance the cycle stability and rate performance of the whole sulfur cathode. It delivers a reversible capacity of 809 mAh g^{-1} after 134 cycles with a high coulombic efficiency (96.6%) and capacity retention (95%) at 0.8 C.

The authors gratefully acknowledge the financial support by the National Natural Science Foundation of China (No. 21376090), the Fundamental Research Funds for the Central Universities (No. 2013ZM0056), and the Scientific Research Foundation of GuangXi University (Grant No. XGZ130963).

Notes and references

[a] *Guangxi Key Laboratory of Petrochemical Resource Processing and Process Intensification Technology, Guangxi University, Nanning 530004, P. R. China. Fax: +86 771 3233 718; Tel: +86 771 3239 697; E-mail: zhaozhenxia@gxu.edu.cn (Z. X. Zhao)*

[b] *Centre for Green Products and Processing Technologies, Guangzhou HKUST Fok Ying Tung Research Institute, Guangzhou 511458, P. R. China. Fax: +86 20 3468 5679; Tel: +86 20 3468 5680; Email: kechengh@ust.hk (G. H. Chen)*

[c] *School of Chemistry and Chemical Engineering, South China University of Technology, Guangzhou, P. R. China; Tel: +86 20 2223 6416; E-mail: cezhli@scut.edu.cn (Z. Li)*

† Electronic Supplementary Information (ESI) available: Experimental details, structure of the MIL-101(Cr) and electrochemical characterization of the MIL-101(Cr)/S composite results. See DOI: 10.1039/b000000x/

1 J. B. Goodenough and K. S. Park, *J. Am. Chem. Soc.*, 2013, **135**, 1167.
2 A. Manthiram, Y. Z. Fu and Y. S. Su, *Acc. Chem. Res.*, 2013, **46**, 1125.
3 W. D. Zhou, Y. C. Yu, H. Chen, F. J. DiSalvo and H. D. Abruna, *J. Am. Chem. Soc.*, 2013, **135**, 16736.
4 S. T. Lu, Y. W. Cheng, X. H. Wu and J. Liu, *Nano Lett.*, 2013, 13, 2485.
5 S. Evers and L. F. Nazar, *Chem. Comm.*, 2012, **48**, 1233; H. W. Chen, W. L. Dong, J. Ge, C. H. Wang, X. D. Wu, W. Lu and L. W. Chen., *Scientific Report*, 2013, **3**, 1910.
6 N. Li, M. Zheng, H. Lu, Z. Hu, C. Shen, X. Chang, G. Ji, J. Cao and Y. Shi, *Chem. Commun.*, 2012, **48**, 4106.
7 G. Y. Zheng, Q. F. Zhang, J. J. Cha, Y. Yang, W. Y. Li, Z. W. Seh and Y. Cui, *Nano Lett.*, 2013, **13**, 1265.
8 K. H. Kim, Y. S. Jun, J. A. Gerbec, K. A. See, G. D. Stucky, H. T. Jung, *Carbon*, 2014, **69**, 543.
9 H. Wang, Y. Yang, Y. Liang, J. T. Robinson, Y. Li, A. Jackson, Y. Cui and H. Dai, *Nano Lett.*, 2011, **11**, 2644.

10 B. Ding, C. Z. Yuan, L. F. Shen, G. Y. Xu, P. Nie, X. G. Zhang, *Chem. Eur. J.*, 2013, **19**, 1013.

11 J. T. Lee, Y. Y. Zhao, S. Thieme, H, Kim, M. Oschatz, L. Borchardt, A. Magasinski, W. Cho, S. Kaskel, G. Yushin, *Adv. Mater.* 2013, **25**, 4573.

12 H. Furukawa, K. E. Corodova, M. O'Keeffe, O. M. Yaghi, Science, 2013, **30**, 6149.

13 R. Demir-Cakan, M. Morcrette, F. Nouar, C. Davoisne, T. Devic, D. Gonbeau, R. Dominko, C. Serre, G. Férey and J. M. Tarascon, *J. Am. Chem. Soc.*, 2011, **133**, 16154.

14 G. Y. Xu, B. Ding, L. F. Shen, P. Nie, J. P. Han and X. G. Zhang. *J. Mater. Chem. A*, 2013, **1**, 4490.

15 H. B. Wu, S. Wei, L. Zhang, R. Xu, H. H. Hng, X. and W. Lou. *Chem. Eur. J.*, 2013, **19**, 10804.

16 X. Y. Zhou, J. Xie, J. Yang, Y. L. Zou, J. J. Tang, S. C. Wang, L. L. Ma, and Q. C. Liao. *J. Power Sources*, 2013, **243**, 993.

17 X. Y. Zhao, J. P. Tu, Y. Lu, J. B. Car, Y. J. Zhang, X. L. Zhang, X. L. Wang and C. D. Gu. *Electrochimica Acta*, 2013, **113**, 256

18 W. Z. Bao, Z. A. Zhang, Y. H. Qu, C. K. Zhou, X. W. Wang and J. Li. *J. Alloys Compounds*, 2014, **582**, 334

19 H. Xu, Y. F. Deng, Z. C. Shi, Y. X. Qian, Y. Z. Meng and G. H. Chen. *J. Mater. Chem. A*, 2013, **1**, 15142.

20 J. Q. Huang, X. F. Liu, Q. Zhang, C. M. Chen, M. Q. Zhao, S. M. Zhang, W. C. Zhu, W. Z. Qian and F. Wei. *Nano Energy*, 2013, **2**, 314

21 G. Férey, C. Mellot-Draznieks, C. Serre, F. Millange, J. Dutour, S. Surblé and I. Margiolaki, *Science*, 2005, **309**, 2040.

22 X. Li, L. Wang, Q. Xia, Z. Liu and Z. Li, *Catal. Commun.*, 2011, **14**, 15.

23 J. Liu, B. Reeja-Jayan and A. Manthiram, *J. Phys. Chem. C*, 2010, **114**, 9528.